Plasticity-led evolution as an intrinsic property of developmental gene regulatory networks

Eden Tian Hwa Ng and Akira R. Kinjo

Department of Mathematics, Faculty of Science,

Universiti Brunei Darussalam, Jalan Tungku Link,

Gadong BE1410, Brunei Darussalam

May 26, 2023

Abstract

The Modern Evolutionary Synthesis seemingly fails to explain how a population can survive a large environmental change. That is, the pre-existence of heritable variants adapted to the novel environment is too opportunistic whereas the search for new adaptive mutations after the environmental change is too slow. Plasticity-led evolution, the process of initial environmental induction of a novel adaptive phenotype followed by genetic accommodation, has been proposed to solve this problem. However, the mechanism enabling plasticity-led evolution is unclear. Here, we propose computational models that exhibit behaviors compatible with plasticity-led evolution by extending the Wagner model of gene regulatory networks. The models exhibit adaptive plastic response and uncovering of cryptic mutations under large environmental changes, followed by genetic accommodation. Moreover, these behaviors are consistently observed over distinct novel environments. We further show that environmental cues, developmental process, and hierarchical regulation cooperatively amplify the above behaviors and accelerate evolution. These observations suggest that plasticity-led evolution is a universal property of complex developmental regulation independent of particular mutations.

Keywords: adaptive plastic response, cryptic genetic variation, developmental bias, genetic accommodation, eco-evo-devo, computer simulation.

Introduction

According to the Modern Evolutionary Synthesis, the standard theory of evolution, all possible phenotypic variation is almost purely explained by genetic variation (1), either ignoring environmental contributions or treating them as noise (2; 3). In this sense, the standard theory is said to be a theory of mutation-led evolution. Therefore, the only means for an individual to survive a large environmental change is to possess mutations that produce a phenotype that is already adapted to the novel environment (Fig. 1**a**). However, natural selection selects phenotypes that are adaptive in the current environment, making the pre-existence of adaptive phenotypes in novel environments highly unlikely (4). If we assume that adaptive variants only appear after the environmental change, then adaptation requires a search for new adaptive mutations, which can be too slow for the population to survive (5).

Phenotypic plasticity, the ability to change the expressed phenotype in response to a change in environmental cues, has been proposed to remedy the above problem because it could produce a phenotype with higher fitness in a novel environment. Phenotypic plasticity arises from the developmental process which integrates genetic and environmental information to generate a phenotype (6–8). Biological experiments suggest that formerly conditionally expressed traits can become constitutively expressed through a process called genetic assimilation (9). Genetic assimilation was later generalized to genetic accommodation to include any adaptive refinement of phenotype regulation (6; 10).

In *plasticity-led evolution*, the novel adaptive phenotype is initially induced by novel environmental cues; and if the novel environment is persistent, then the novel phenotype undergoes genetic accommodation (6; 12; 13) (Fig. 1**b**). This has been deemed to resolve the problem of gradualism implied by mutation-led evolution (11). Levis and Pfennig proposed the following four criteria for plasticity-led evolution (12):

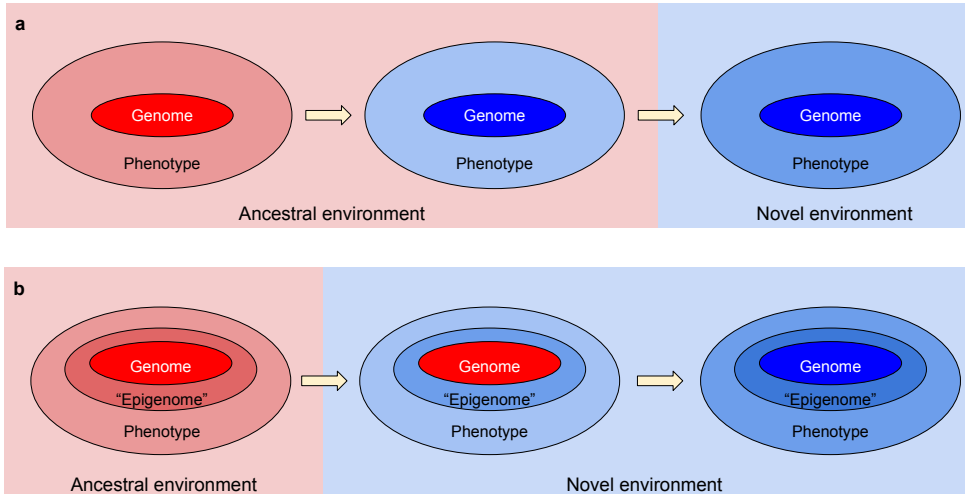

Figure 1: **Comparing different evolutionary theories.** **(a)** In the standard theory of evolution, novel phenotypes are induced by mutations. If the novel phenotype has a fitness benefit in the novel environment, it gets favored by selection. **(b)** In plasticity-led evolution, novel phenotypes are induced by environmental change via phenotypic plasticity without a change in the genome. Here, the "epigenome" refers to the whole set of mechanisms that regulate gene expressions and development, thereby mediating phenotypic plasticity (11). If the novel environment is persistent, genetic accommodation refines the novel phenotype into a higher quality form.

1. The novel adaptive phenotype is initially induced by plasticity.
2. Cryptic mutations are uncovered as a result of the plastic response.
3. The phenotype undergoes a change in regulation.
4. The phenotype undergoes adaptive refinement under selection.

There are numerous studies on natural populations to evaluate whether plasticity-led evolution has occurred (12). However, the mechanisms by which plasticity-led evolution is made possible remain unclear, resulting in misunderstanding and confusion on the meaning and implications of plasticity-led evolution (1; 10; 13; 14). For example, if plastic responses are regulated by particular genes, plasticity itself may be subject to natural selection. The "plasticity-led evolution" based on such gene-regulated plasticity is therefore still within the framework of Modern Evolutionary Synthesis, and hence the problem of gradualism remains. This suggests that plasticity in plasticity-led evolution should emerge from non-genetic causes (5; 11). But what can they be? It has been suggested that the evolutionary capacitance, buffering of genetic variation under adapted environments, is a general feature of complex gene regulatory networks (GRNs), rather than particular mutations (15).

In a similar manner, can plastic response to environmental change be a general feature of GRNs?

To pursue this possibility, we study computational models of evolutionary developmental systems. Such models should be able to express changes in phenotype in response to changes in environmental cues, possess a developmental framework as well as hierarchical regulation (16; 17). In plasticity-led evolution, the environment encountered by a population plays two roles. One induces phenotypic response (environment-as-inducer) and the other selects phenotypes more adapted to it (environment-as-selector). There are existing works that incorporate some aspects of phenotypic response to different environmental cues (18–20). However, so far there seem to be no studies that explicitly correlate the two roles of the environment (4). The developmental process is often overlooked in traditional quantitative genetics models and their extensions because it does not directly contribute to phenotypic variation (3; 21; 22). However, it is an essential process that integrates environmental and genetic information into phenotype (6; 7). Biological gene regulatory networks have a hierarchical organization (16; 17). However, all studies of computational models ignore this biological aspect of development (except for Ref. (23), but it lacks developmental regulation).

We demonstrate that models that include all the above ingredients satisfy the Levis-Pfennig criteria for plasticity-led evolution (12). We also demonstrate how each of these ingredients cooperatively enhance adaptation and accelerate evolution. We further show that these models exhibit plasticity-led evolution as a generic feature independent of specific mutations or particular environmental changes.

Modelling

A computational model of plasticity-led evolution should incorporate several core notions: environment (-as-inducer and -as-selector), gene regulatory network, developmental process, selection, and reproduction. The environment-as-inducer represents the role of the environmental cue in determining phenotype alongside the genome. The environment-as-selector represents the role of the environment as a selection agent. We assume, in our work, that these two roles of the environment are highly correlated. The gene regulatory network represents regulation of pheno-

type expression through gene-gene and gene-environment interactions. We model the developmental process as the recursive regulation of gene expressions over time to express the phenotype. Selection favors individuals that have adult phenotypes that better match the environment-as-selector. Selected individuals then reproduce. That is, their genomes are recombined and mutated to produce the next generation of individuals.

A minimal model that incorporate all these notions is a recursive gene regulatory network introduced by A. Wagner (24). In the Wagner model, the gene expression at the s-th stage of development is represented by a vector $g(s)$. The genome is represented by a matrix G where the (i, j) element represents regulatory effect of the j-th gene on the i-th gene.

$$g_i(s) = \sigma\left(\sum_j G_{ij} g_j(s-1)\right) \tag{1}$$

where σ is an activation function.

The developmental process is naturally represented by the sequence of vectors $g(0), g(1), g(2), \cdots$. The phenotype of the individual is usually taken as the steady state of Eq.(1) if it converges. The Wagner model has been used to demonstrate evolution of mutational robustness (24), evolutionary capacitance (15), the link between mutational and environmental robustness (25), the role of robustness in evolution (26; 27), the role of phenotypic plasticity in directing evolution (28) and the emergence of bistability (19; 20). These works in fact provide indirect evidence suggesting that the Wagner model exhibits plasticity-led evolution (4).

However, previous works using the Wagner model did not include correlations between the environment-as-inducer and environment-as-selector to validate whether plastic response is adaptive. These works also do not emphasize the roles of developmental process or hierarchical regulation of GRNs. We therefore extend the Wagner model by introducing these extra features.

Macro-environment and environmental cues

We remind that the environment plays two roles in eco-evo-devo biology. The "environment-as-inducer" forms a cue integrated into phenotype expression. The

Table 1: Summary of parameters in model variants. dim g is the dimension of the g vector. All other vectors, if present, are 200-dimensional. Matrix densities $(\rho_G, \rho_P, \rho_E, \rho_H)$ are chosen to ensure that the number of non-zero elements are equal between different models on average. Our study used $\rho_0 = 0.02$.

	Full	NoHier	NoCue	NoDev
vectors	$e-p, f, g, h, p$	$e-p, g, p$	$-p, f, g, h, p$	e, f, g, h, p
matrices	E, F, G, H, J, P	E, G, P	E, F, G, H, J, P	E, F, G, H, P
dim g	200	600	200	200
ρ_G	ρ_0	$4\rho_0/9$	ρ_0	ρ_0
ρ_P	ρ_0	$\rho_0/3$	ρ_0	ρ_0
ρ_E	ρ_0	$\rho_0/3$	ρ_0	ρ_0
ρ_H	ρ_0	N.A.	ρ_0	$2\rho_0$

"environment-as-selector" determines the fitness of adult individuals. Previous works using the Wagner model do incorporate these notions of the environment but did not enforce correlations between these two roles. We define the macro-environment as a 200-dimensional vector $\mathbf{e}$ representing the average environment exerted on the population. Each element of $\mathbf{e}$ takes a value of 1 or -1. We modeled the environmental cue e of each individual as the macro-environment $\mathbf{e}$ with noise by randomly flipping 5% of elements of $\mathbf{e}$. This environmental cue e may be considered as the micro-environment of an individual.

Genome and developmental process

We now introduce several variants of the Wagner model. The *Full* model (Fig. 2**a**) is the main focus of this study which incorporates response to environmental cues, developmental process and hierarchical regulation. As control, we also introduce *NoHier*, *NoCue*, *NoDev* (Fig. 2**b-d**) models to highlight the role of each of these ingredients in plasticity-led evolution.

Full Model

We introduce a vector $p(s)$ representing the phenotype expressed at the s-th stage of development and $\tilde{p}(s)$ as the exponential moving average of the phenotype (see **Methods**). To reflect hierarchical regulation of GRN elements (such as epigenetic marks, RNAs and proteins), we further introduce a layer of vector $f(s)$ to represent epigenetic marks, and a layer of vector $h(s)$ to represent higher-order complexes (such as proteins, supramolecular complexes etc.). Thus, we assume the following

mutually recursive equations:

$$
\begin{aligned}
f_i(s) &= \sigma_f \left(\sum_{j=1}^{200} G_{ij} g_j(s-1) + \sum_{j=1}^{200} E_{ij}(e_j - \tilde{p}_j(s-1)) \right), \\
g_i(s) &= \sigma_g \left(\sum_{j=1}^{200} F_{ij} f_j(s) \right), \\
h_i(s) &= \sigma_h \left(\sum_{j=1}^{200} H_{ij} g_j(s) + \sum_{j=1}^{200} J_{ij} h_j(s-1) \right), \\
p_i(s) &= \sigma_p \left(\sum_{j=1}^{200} P_{ij} h_j(s) \right),
\end{aligned}
\tag{2}
$$

where E is a matrix that represents environmental regulation of epigenetic marks, F is a matrix representing epigenetic regulation of gene expression levels, G is a matrix representing genetic regulation of epigenetic marks, H is a matrix representing genetic regulation of higher-order complexes, J is a matrix representing interactions among higher-order complexes, P is a matrix representing regulation of the phenotype. The matrix ensemble E, F, G, H, J, P therefore represents the genome of the individual. We set the base matrix density as $\rho_0 = 0.02$, which is the density of each matrix in the Full model. The matrix densities for the other models are determined such that the number of nonzero mutations are equal between different models on average. $\sigma_f, \sigma_g, \sigma_h, \sigma_p$ are activation functions based on arctangent or hyperbolic tangent functions. The initial conditions are set to $f(0) = \mathbf{0}$, $g(0) = \mathbf{1}$, $h(0) = \mathbf{0}$ and $p(0) = \mathbf{0}$ where $\mathbf{0}$ is the zero vector and $\mathbf{1}$ is a vector where all elements are equal to 1. $f(s), g(s), h(s), p(s)$ are all 200-dimensional vectors in the Full model. We iteratively compute the state vectors $f(s), g(s), h(s), p(s)$ for $s = 1, 2, \cdots$ until the phenotype $p(s)$ converges (see **Methods**). Note that the environmental cues are fed to the system as $e - p(s)$ rather than e per se. As explained below, (selected elements of) p approaches $\mathbf{e}$, and hence (selected elements of) $e - p$ converges to $\mathbf{0}$ (except for the noise part), as the population adapts towards $\mathbf{e}$. In other words, the effect of the environmental cues decreases as adaptedness increases. In this way, we expect to model genetic assimilation.

NoHier model

To study the effect of hierarchical structure on GRNs, we introduce a developmental model without a hierarchical structure, which we name the *NoHier* model (Fig. 2**b**):

$$
\begin{aligned}
g_i(s) &= \sigma_g \left(\sum_{j=1}^{600} G_{ij} g_j(s-1) + \sum_{j=1}^{200} E_{ij}(e_j - \tilde{p}_j(s-1)) \right), \\
p_i(s) &= \sigma_p \left(\sum_{j=1}^{600} P_{ij} g_j(s) \right).
\end{aligned}
\tag{3}
$$

To preserve the degrees of freedom between the Full and NoHier models, the vector representing gene expression levels $g(s)$ is set to 600-dimensional for the NoHier model and its matrix densities are adjusted accordingly (Table 1). The dimensions of vectors representing the environment e and phenotype $p(s)$, are kept at 200.

NoCue model

To study the effect of environmental cues on development, we introduce a developmental model where the environmental cue e is absent in development, which we name the *NoCue* model (Fig. 2**c**):

$$
\begin{aligned}
f_i(s) &= \sigma_f \left(\sum_{j=1}^{200} G_{ij} g_j(s-1) - \sum_{j=1}^{200} E_{ij} \tilde{p}_j(s-1) \right), \\
g_i(s) &= \sigma_g \left(\sum_{j=1}^{200} F_{ij} f_j(s) \right), \\
h_i(s) &= \sigma_h \left(\sum_{j=1}^{200} H_{ij} g_j(s) + \sum_{j=1}^{200} J_{ij} h_j(s-1) \right), \\
p_i(s) &= \sigma_p \left(\sum_{j=1}^{200} P_{ij} h_j(s) \right).
\end{aligned}
\tag{4}
$$

Apart from the absence of the vector e, this is identical to the Full model.

NoDev model

To highlight the importance of the developmental process, we use the Full model described by Eq. (2) but set the maximum number of developmental steps to 1 for

minimal development. We name this the *NoDev* model (Fig. 2**d**):

$$
\begin{aligned}
f_i(1) &= \sigma_f \left(\sum_{j=1}^{200} G_{ij} g_j(0) + \sum_{j=1}^{200} E_{ij} e_j \right), \\
g_i(1) &= \sigma_g \left(\sum_{j=1}^{200} F_{ij} f_j(1) \right), \\
h_i(1) &= \sigma_h \left(\sum_{j=1}^{200} H_{ij} g_j(1) \right), \\
p_i(1) &= \sigma_p \left(\sum_{j=1}^{200} P_{ij} h_j(1) \right).
\end{aligned}
\tag{5}
$$

Hence, $p(1)$ is immediately taken as the adult phenotype. To compensate for the absence of self-regulation of the h layer, we double the density of the H matrix (Table 1).

Natural selection and reproduction

We impose the role of the environment-as-selector by evaluating the fitness of each individual by matching the macro-environment $\mathbf{e}$ with the adult phenotype p (assuming that p converges). We also included the number of developmental steps up to convergence into the calculation of fitness such that individuals with a lower number of developmental steps are favored. We define the raw fitness of the i-th individual as:

$$
\omega_i = \exp(-(\alpha \|p - \mathbf{e}\|_1 + \beta N_{\text{step}})) \tag{6}
$$

where $\|p - \mathbf{e}\|_1$ is the absolute (L1) distance between the first 40 (out of 200) elements of the adult phenotype p and the corresponding elements of the macro-environment $\mathbf{e}$, N_{step} is the number of developmental steps until convergence, α and β are positive constants. In other words, only 40 traits (elements of the phenotype vector) are subject to selection, and other $160 (= 200 - 40)$ traits are allowed to evolve freely. In this paper, we call the value of $\|p - \mathbf{e}\|_1$ mismatch. Individuals whose phenotype $p(s)$ does not converge before a pre-specified number (200) of steps are given a fitness of zero. The population in which all individuals have completed the developmental process is called the adult population in the following. The

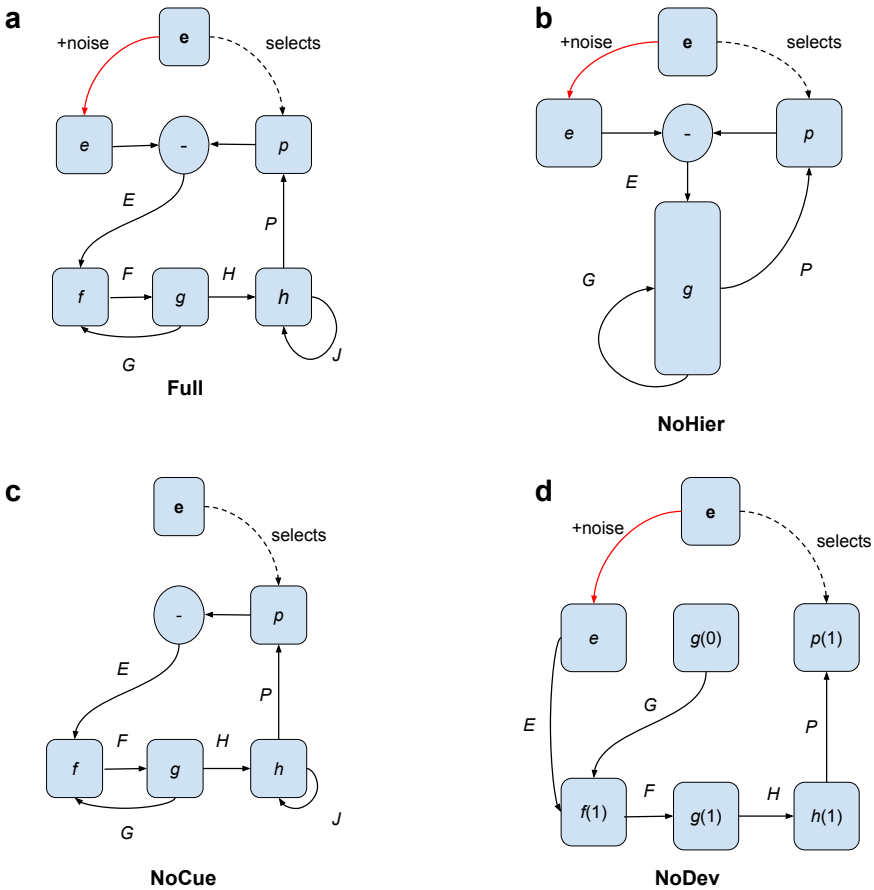

Figure 2: **Diagram representing regulation between different layers of different models.** Boldface **e** represents the macro-environment. e, f, g, h, p represent vectors. Black solid arrows represent regulatory interactions. Red solid arrow represents noise. Black dotted arrow represents selection. E, F, G, H, J, P represent regulatory matrices . **(a)** Full model (Eq.. 2); **(b)** NoHier (Eq. 3); **(c)** NoCue (Eq. 4); **(d)** NoDev (Eq. 5).

normalized fitness of the i-th individual of the adult population is given by

$$\Omega_i = \frac{\omega_i}{\max_j\{\omega_j\}} \tag{7}$$

where $\max_j\{\omega_j\}$ is the maximum raw fitness of the adult population.

The offsprings of individuals are generated as follows:

1. Initialize the selected population as an empty set.
2. Uniformly sample individual i from the adult population.
3. Sample a random number r from the uniform distribution between 0 and 1.
4. If $r < \Omega_i$, then a copy of the i-th individual is added to the selected population.
5. The i-th individual is replaced back to the adult population.
6. Repeat steps 2-5 until the size of the selected population reaches the maximum population size of 1000 individuals.
7. Individuals i and $i+1$ where $i = 1, 3, 5, \cdots$ of the selected population are paired to become parents.
8. For each pair of parents, two offsprings are produced by randomly shuffling the corresponding rows of the genome matrices with probability 0.5 between the parents.
9. The genome matrices of the offsprings are mutated with a given probability (see **Methods**).

Adaptive evolution of a population in an environment is therefore modeled by repeated cycles of development, selection and reproduction under the given environment.

Simulating plasticity-led evolution

To study plasticity-led evolution, we require at least two environments: the ancestral environment, to which the population is adapted, and the novel environment, to which the population is to adapt. To let the population adapt to an environment, we simulate adaptive evolution for 200 generations. We call this duration an *epoch*, and it is considered a unit of evolutionary time-scale. In each epoch, the macro-environment is set constant. For each model, we first simulated adaptive

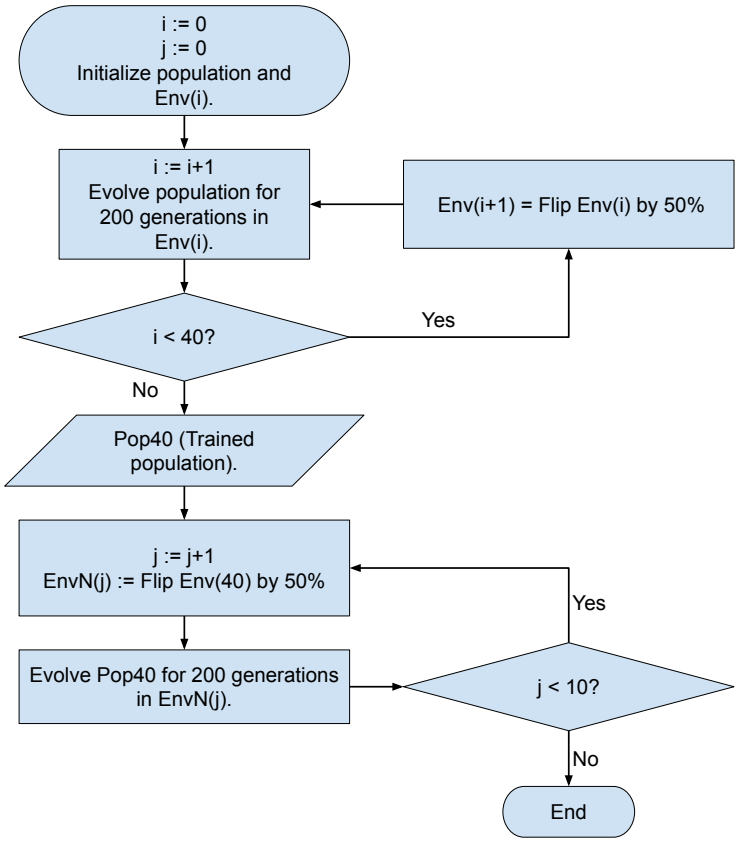

Figure 3: **Simulating plasticity-led evolution.** During each training epoch, populations of individuals are subjected to selection. Each epoch lasts for 200 generations. At the end of each training epoch, the macro-environment is changed by randomly flipping 50% of the environmental factors. This process is repeated so that the population is subject to selection under 40 different environments in turn. After training for 40 epochs, the population is subject to selection in the novel environment which is generated by flipping 50% of the environmental factors of the final training environment. Evolution is tracked in 10 different novel environments to assess quality of evolution with respect to plasticity-led criteria.

evolution for 40 epochs in turn. Between two consecutive epochs, we introduce a large environmental change by randomly flipping 50% of the elements of the macro-environment vector $\mathbf{e}$. We take the macro-environment of the 40-th epoch as the ancestral environment for subsequent epochs.

After adapting to the ancestral environment, we introduce a large environmental change by randomly flipping 50% of the elements of the ancestral macro-environment vector to generate a novel environment. We subject the population to selection under the novel environment for one epoch and assessed its adaptation. We repeat this 10 times with different novel environments.

Results

We first present a visualization of the trajectory of the phenotype and genotype over evolution. By looking at the initial phase of the trajectory, we assess plastic response and uncovering of cryptic mutations. The visualization also lets us track adaptive change in mean value and variation of genotype and phenotype over evolution. We compared different models in light of the Levis-Pfennig criteria of plasticity-led evolution (12). We also present additional results closely related to plasticity-led evolution: developmental bias, evolutionary capacitance and developmental memory.

Visualizing evolution: The Genotype-Phenotype plot

To visualize evolution, we plotted the phenotypic value in the ancestral and novel environments against the genotypic value of the population over evolution. We call this plot the *genotype-phenotype plot* (Fig. 4). Here, the phenotypic value is computed by projecting the phenotype vector onto an axis where a value of 0 means that the adult phenotype is perfectly adapted to the ancestral environment and a value of 1 means that it is perfectly adapted to the novel environment. Similarly, the genotypic value is computed by projecting the genome matrices (construed as a vector) onto an axis where a value of 0 represents the population average of genotype adapted to the ancestral environment and a value of 1 represents the population average of genotype after adapting to the novel environment for an epoch (see **Methods**). Therefore, the trajectory of adaptive evolution in the novel environment generally proceeds from the lower left corner to the upper right corner in the genotype-phenotype plot.

From the genotype-phenotype plots, we observe that all discussed models are capable of adaptive evolution. The projected value of the novel phenotype tends to increase as the projected value of genotype increases. The final average value of the projected phenotype for all models is about 1 in the novel environment after an epoch, indicating adaptation.

For the Full and NoHier models (Fig. 4 **a**,**b**), the phenotypes induced by the novel environment show substantially larger projected values than the phenotypes induced by the ancestral environment in the first generation. This indicates adap-

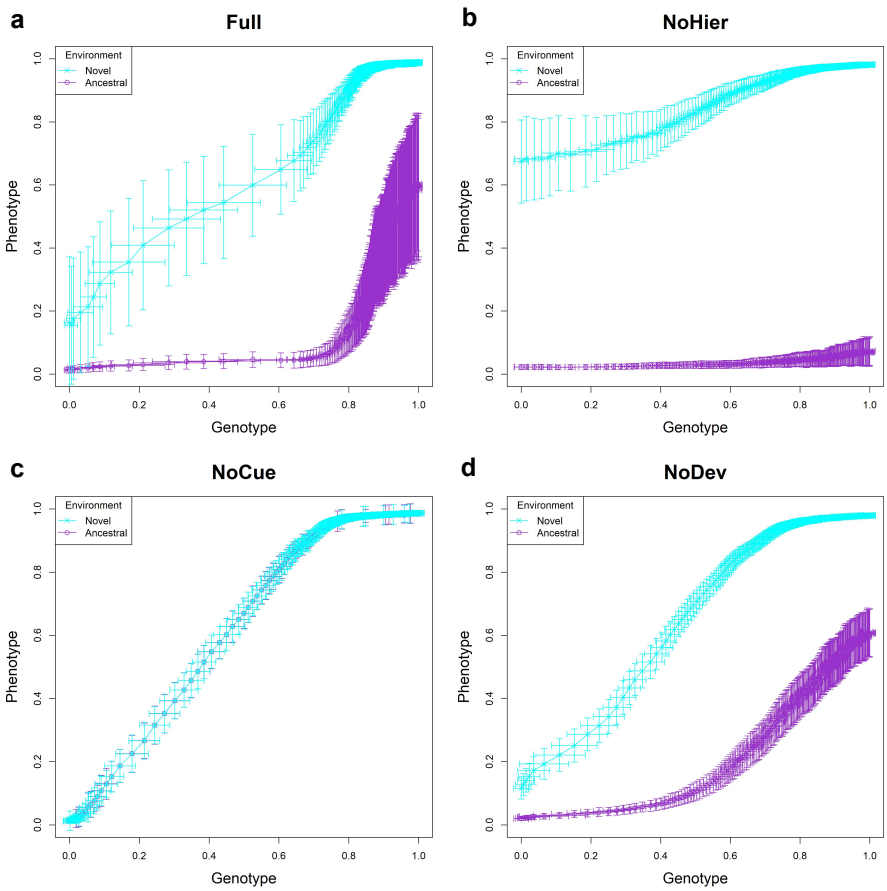

Figure 4: **Trajectory of projected phenotype against projected genotype.** Each point represents the population average of genotypic value (horizontal axis) and phenotypic value (vertical axis) at each generation (error bars represent respective standard deviations). Cyan and purple represent populations in novel and ancestral environments, respectively. Projected phenotypic values of 0 and 1 correspond to perfectly fit phenotypes in ancestral and novel environments, respectively. Projected genotypic values of 0 and 1 correspond to the population average genome at 1st and 200th generations, respectively. Hence, the trajectory generally proceeds from the lower left corner to the upper right corner. **(a)** Full model; **(b)** NoHier; **(c)** NoCue; **(d)** NoDev. See also Supplementary Information.

tive plastic response. The standard deviation in phenotype in the novel environment is much larger than that in the ancestral environment in the first generation. This can be due to uncovering of cryptic mutations or the amplification of the phenotypic response to environmental noise. However, a higher rate of change of projected genotype observed in Full and NoHier models during the early stages of adaptation indicates rapid purification of heritable variation during that phase. This suggests that the large standard deviation is more likely due to uncovering of cryptic mutations (but see subsection **Environmental and genetic variations induce correlated phenotypic variation** below). Notable differences between Full and NoHier models are (1) the much larger standard deviation in ancestral phenotypic

values in the Full model after adaptation, and (2) lower ancestral phenotypic values in the NoHier model after adaptation (see also Supplementary Information). The latter point indicates that the NoHier model is more overfitted to the ancestral environment.

In the NoCue model (Fig. 4 **c**), the environmental cues are absent in development. Consequently, there is no phenotypic plasticity, and the phenotypes expressed in the ancestral and novel environments are almost identical. The slight difference in phenotypes in the genotype-phenotype plot is purely due to the difference in mutations. The early stage of adaptation is very slow, as seen in the cluttered distribution of points in the lower left corner. This is followed by a rapid change in genotype, as seen in the sparse distribution of points around the center of the plot. This observation demonstrates that evolution in novel environments in the absence of phenotypic plasticity is characterized by an initial slow change followed by rapid adaptation once adaptive mutations appear.

In the NoDev model (Fig. 4 **d**), we observe some adaptive plastic response. However, this adaptive plastic response is smaller than those of the Full or NoHier models on average. Similarly there is less difference in the standard deviation in phenotypes between environments compared to the Full or NoHier models, indicating less uncovering of cryptic mutations. These observations highlight the importance of the developmental process in plasticity-led evolution.

We provide additional genotype-phenotype plots for different novel environments in Supplementary Information. We observe that these behaviors are consistent over different novel environments.

Initial plastic response tends to be adaptive

On the genotype-phenotype plots (Fig. 4), plastic responses are observed as a vertical shift between the ancestral and novel environments in the same generation. If the projected phenotype in the novel environment is greater than that in the ancestral environment, then the plastic response is adaptive. We examined this shift in projected phenotype to detect adaptive plastic response (Fig. 5 **a**). The Full and NoHier models exhibit large adaptive plastic responses on average. The NoDev model exhibits some adaptive plastic response, but it is not as large as those

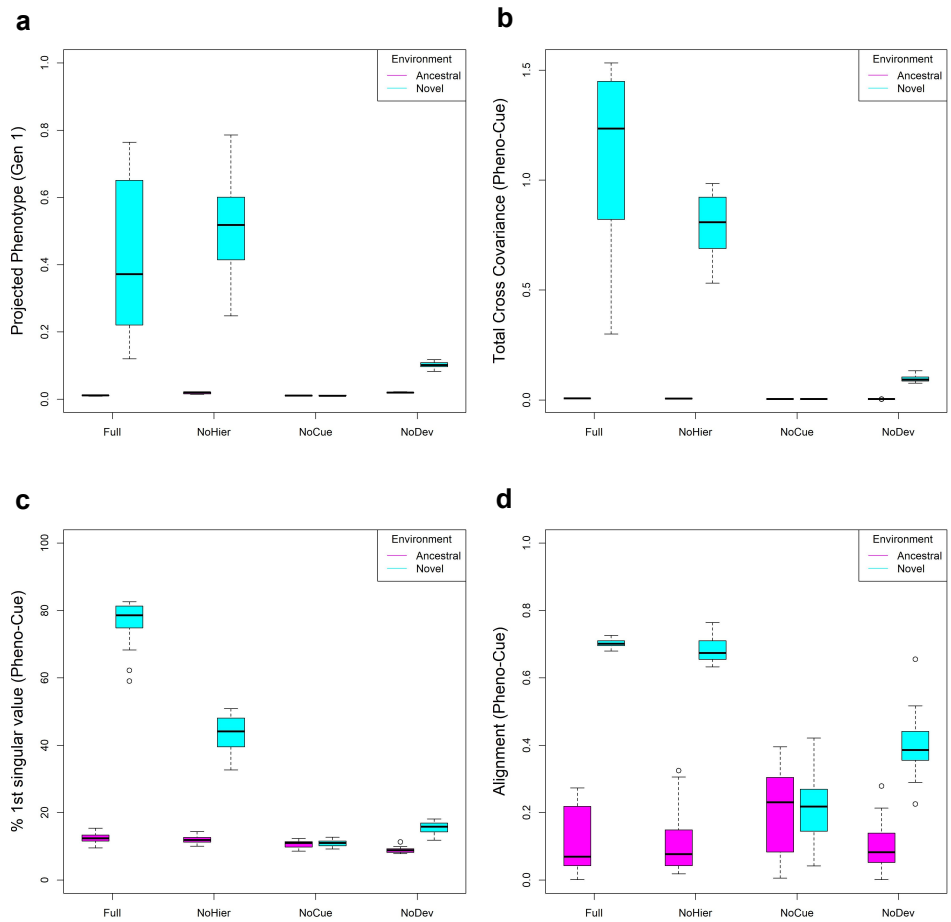

Figure 5: **Adaptive plastic response in the first generation.** **(a)** Boxplot of projected phenotype under ancestral and novel environment. **(b)** Boxplot of total cross-covariance between phenotype and environmental cue. **(c)** Boxplot of percentage contribution of the first singular value of the cross-covariance matrix to the total cross-covariance between phenotype and environmental cue. **(d)** Boxplot of alignment between phenotype variation and environmental change, where the alignment is the correlation between the first phenotype singular vector with respect to environmental variation and the direction of environmental change.

in the Full and NoHier models. As expected, the NoCue model does not exhibit any plastic response.

To analyze the correlation between phenotype and environmental cues immediately after large environmental changes, we computed their cross-covariance matrix in the first generation, which we call the Pheno-Cue cross-covariance matrix. We performed singular value decomposition (SVD) on the Pheno-Cue cross-covariance matrix to find the principal components (see **Methods**). The left singular vectors correspond to the principal axes of phenotypes, the right singular vectors correspond to the principal axes of environmental cues, and the singular values correspond to the cross-covariance between the corresponding left and right principal components.

We performed this analysis for each model under ancestral and novel environments.

We observed a larger total cross-covariance between phenotypes and environmental cues in the novel environments than in the ancestral environment (Fig. 5 **b**). This suggests that populations are generally far more sensitive to environmental noise under novel environments than under the ancestral environment. Among all models, the Full model has the largest cross-covariance, followed by the NoHier model. This suggests that a hierarchical structure in GRNs exaggerates phenotypic variation due to environmental noise. NoCue has little cross-covariance because the model itself is insensitive to environmental cues. NoDev exhibits smaller cross-covariances than the Full and NoHier models. This demonstrates that the developmental process amplifies variation in phenotype due to environmental noise in novel environments.

Previous works suggest that if the phenotypic variation is developmentally biased in line with the environmental change, then such developmental bias, i.e., the tendency to generate certain phenotypes more readily than others, can facilitate evolution in novel environments (29; 30). To detect any developmental bias in our models, we examined the proportion of the first singular component for each model under ancestral and novel environments. Fig. 5 (**c**) shows that the proportion of the first singular value tends to be larger in the novel environment than in the ancestral environment. This indicates that the phenotypic variation due to environmental noise is more biased in the direction of the first principal component in the novel environment. In particular, the Full model exhibits the greatest bias in phenotypic variation, followed by NoHier, in the novel environment. This shows that hierarchical regulation enhances developmental bias. The NoCue and NoDev models exhibit little bias in the novel environment. For the NoCue model, this is easily explained by the absence of environmental cues. For the NoDev model, this result emphasizes that the developmental process is essential in generating developmental bias. On the other hand, all models exhibit small developmental biases in the ancestral environment. Together with the small total cross-covariances (Fig. b), this implies that all models are extremely robust against environmental noise in adapted environments (26).

To see if the above developmental bias is aligned with environmental change,

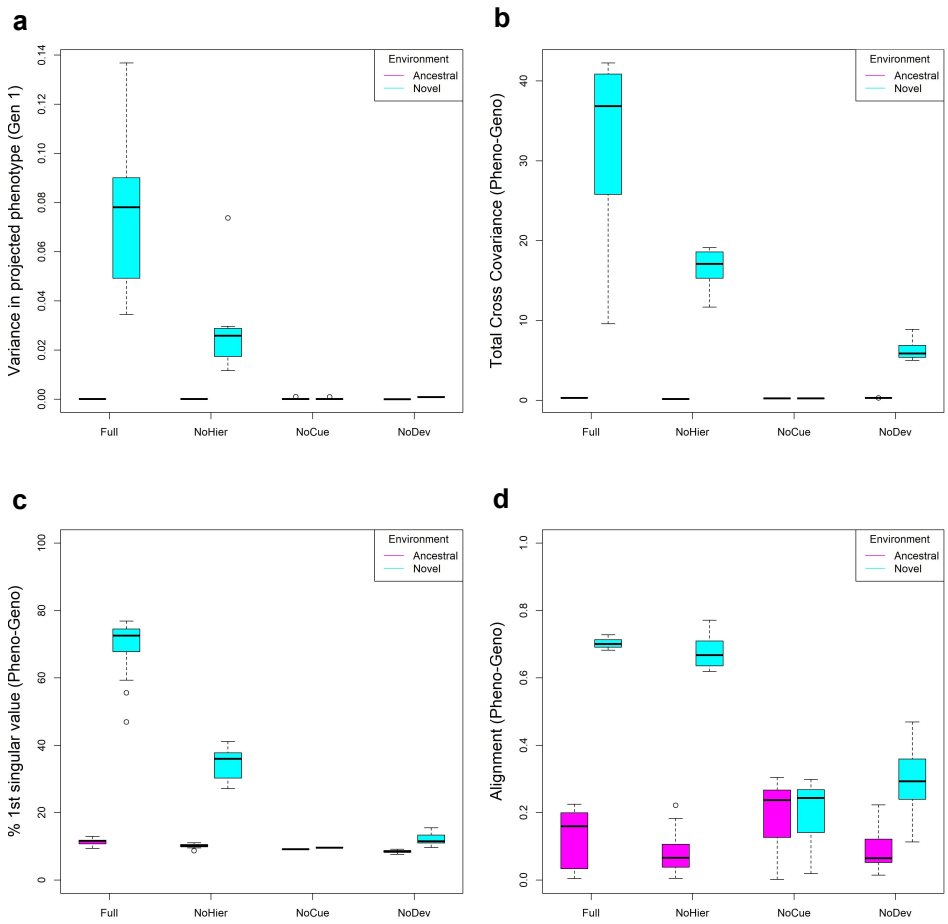

Figure 6: **Uncovering of cryptic mutations.** **(a)** Boxplot of variance in projected phenotype in ancestral and novel environments. **(b)** Boxplot of total cross-covariance (square of Frobenius norm) between phenotype and genome. **(c)** Boxplot of percentage contribution of the first singular value of the cross-covariance matrix to total cross-covariance between phenotype and genome. **(d)** Boxplot of alignment between phenotype variation and environmental change, where the alignment is the correlation between the first phenotype singular vector with respect to genetic variation and the direction of environmental change. Variation due to mutations and environmental noise are very similar qualitatively (c.f. Fig. 5).

we computed the correlation between the first phenotype singular vector and the direction of environmental change (Fig. 5 **d**). The Full and NoHier models exhibit good alignment (roughly 0.7), with NoHier exhibiting larger variance in alignment. Given the small proportions of the first singular values, the correlations for the NoCue and NoDev models are insignificant.

Developmental process uncovers cryptic mutations

As we mentioned above (**Visualizing evolution: The Genotype-Phenotype plot**), the large phenotypic variation in the novel environment compared to the

ancestral environment during the early phase of evolution is most likely due to uncovering of cryptic mutations (Fig. 4). We compared the magnitude of variance in projected phenotypes between ancestral and novel environments (Fig. 6 **a**). We observed small variance in projected phenotype in every model in the ancestral environment. This can be explained by the evolved robustness in adapted environments (15; 19; 20; 24–26; 31). The Full model exhibits the largest variance of projected phenotype in the novel environment on average, followed by the NoHier model, indicating that hierarchical regulation amplifies the effects of genetic variation. Compared to these, the NoDev model exhibits smaller variance in projected phenotype in the novel environment. This indicates that developmental process plays a critical role in uncovering cryptic mutations. The NoCue model does not exhibit any difference in projected phenotype because environmental cues is necessary for uncovering of cryptic mutations.

To analyze the phenotypic variation due to mutations, we calculated the cross-covariance between the phenotype and the genome, which we call the Pheno-Geno cross-covariance matrix (see **Methods**). As we did for the Pheno-Cue cross-covariance matrix in the previous subsection, we performed SVD analysis on the Pheno-Geno cross-covariance matrix. Here, the right singular vectors correspond to principal axes of mutations instead of environmental cues.

We notice that the SVD analysis on the Pheno-Geno cross-covariance (Fig. 6**b-d**) is qualitatively similar to that on the Pheno-Cue cross-covariance (Fig. 5**b-d**). That is, the Full and NoHier models exhibit large total cross-covariances between phenotype and mutation (Fig. 6**b**), their phenotypic variation due to mutations are highly biased in novel environments (Fig. 6**c**), and that phenotypic variations are biased in the direction of environmental change (Fig. 6**d**). On the other hand, NoDev and NoCue models have smaller total cross-covariance (Fig. 6**b**) and lack developmental bias (Fig. 6**c,d**).

Environmental and genetic variations induce correlated phenotypic variation

We observed that the results from SVD analysis on the Pheno-Cue cross-covariance matrix are qualitatively similar to that with the Pheno-Geno cross-covariance ma-

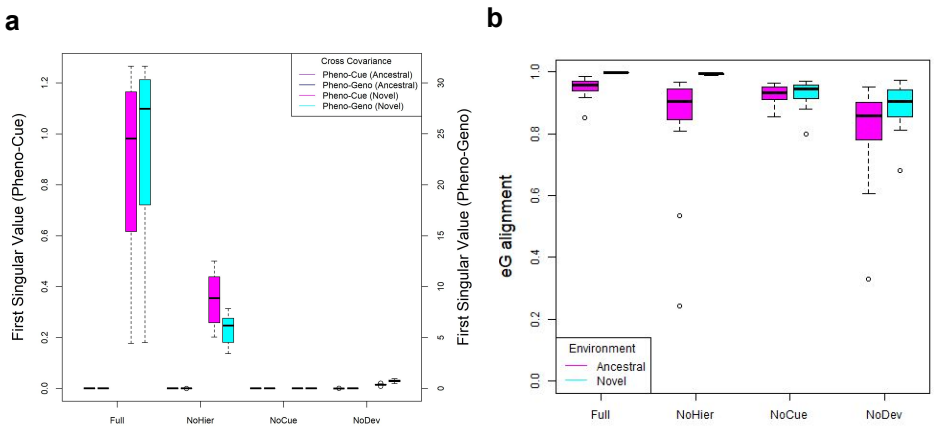

Figure 7: **Environmental variation and genetic variation induce correlated phenotypic variation**. **(a)** Boxplot of first singular values of Pheno-Cue and Pheno-Geno cross-covariance matrices in ancestral and novel environments. **(b)** Boxplot of Pheno(Cue)-Pheno(Geno) alignment; calculated as the correlation between the first singular vector of the Pheno-Cue cross-covariance matrix and the first singular vector of the Pheno-Geno cross-covariance matrix.

trix, leading to similar conclusions (c.f. Figs. 5 and 6). To examine the correlation between the phenotypic variation due to environmental noise and that due to mutations, we compared the first singular values of the Pheno-Cue and Pheno-Geno cross-covariance matrices (Fig. 7**a**). The distribution of the first singular values over different models is qualitatively similar between the Pheno-Cue and Pheno-Geno cross-covariances. That is, the first singular values decrease in the order of Full, NoHier, NoDev and NoCue models in the novel environments, whereas all models exhibit very small first singular values in the ancestral environment. Quantitatively, the first singular values of the Pheno-Geno cross-covariance matrices (right vertical axis of Fig. 7**a**) are much greater than those of the Pheno-Cue cross-covariance matrices (left vertical axis of Fig. 7**a**). This is because the number of elements of the genome vector is much larger than that of the environmental cue vector.

We next calculated the correlation between the first singular vector of the Pheno-Cue cross-covariance matrix and that of the Pheno-Geno cross-covariance matrix to see the alignment between them (Fig. 7**b**). These axes are highly correlated, especially in the novel environment. In particular, the Full and NoHier models have almost perfect alignment in the novel environment. We remark that the apparent high correlations in all other cases are spurious because the phenotypic distributions of these populations are unbiased (c.f. low percentage of first singular values from

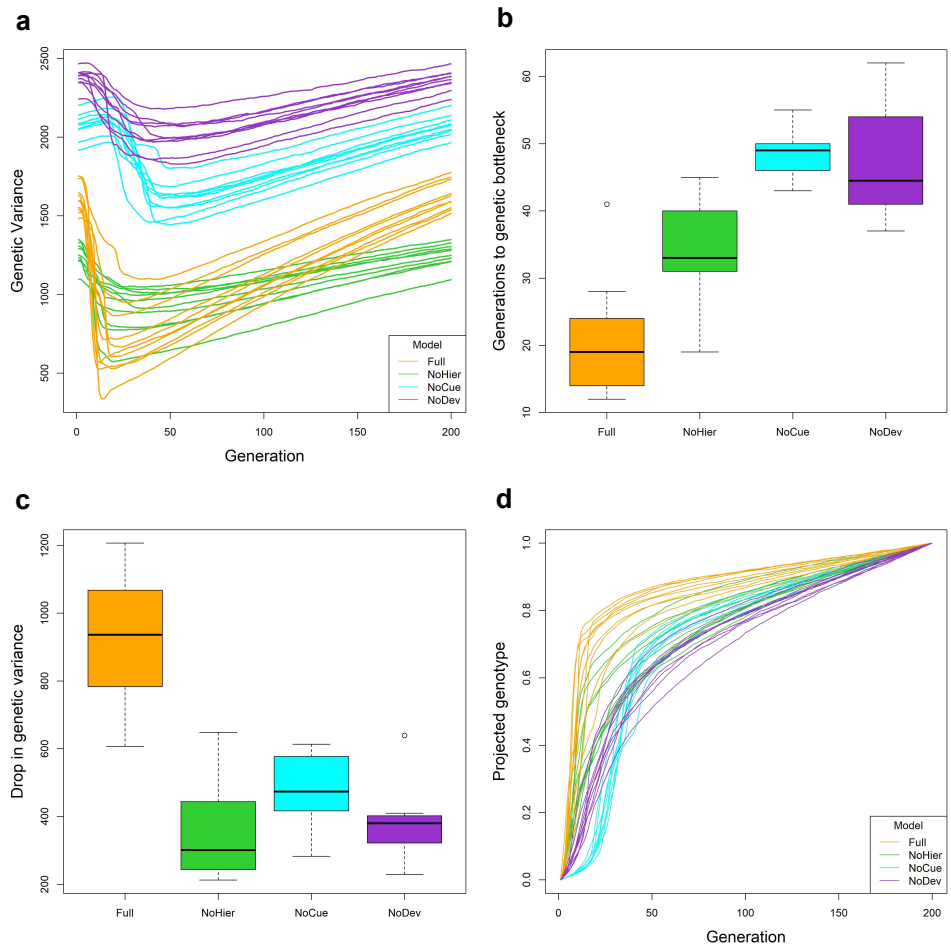

Figure 8: **Change in regulation.** **(a)** Trajectory of genetic variance over evolution. **(b)** Boxplot of number of generations to genetic bottleneck, where the genetic bottleneck is the generation when the genetic variance is minimum (c.f. panel **a**). **(c)** Boxplot of drop in genetic variance between generation 1 and the genetic bottleneck. **(d)** Trajectory of projected genotype over evolution.

Fig. 5**c** and 6**c**) and the spurious correlation is due to the idiosyncrasies of the SVD algorithm used rather than actual good alignment. These observations show that our models can reproduce existing results in literature which demonstrate the interchangeability of environmental and mutational perturbations in producing phenotypes (6; 25; 32; 33).

Full model exhibits fastest change in regulation

To study the change in regulation, or the reorganization of the genome, we track the genetic variance (i.e. the sum of the variance in each element of the genome matrices) over evolution (Fig. 8**a**). A rapid decrease in genetic variance means strong purifying selection. A gradual increase in genetic variance means accumulation of neutral or beneficial mutations. The Full and NoHier models immediately experi-

ence strong selection in the novel environment, with the Full model experiencing the most stringent selection (largest decrease in the shortest time). The NoDev model experiences weaker selection than the Full and NoHier models. In contrast to the other models, the genetic variance of the NoCue model first increases slightly and then decreases rapidly before gradually increasing again. The initial increase in genetic variation in the NoCue model may be attributed to the search for adaptive mutations in the novel environment.

The genetic variance of the NoDev model is consistently greater than those of all the other models. Due to the lack of development, the NoDev model cannot fully express genetic variation in phenotype. Hence, selection cannot effectively purify the genetic variation. The genetic variance of the NoCue model is slightly smaller than that of the NoDev model, but consistently greater than those of the Full and NoHier models. This suggests that most of the mutations are latent in the NoCue model, which in turn highlights the role of environmental cues in uncovering cryptic mutations.

We define the genetic bottleneck as the generation when the genetic variance is minimum (c.f. Fig. 8**a**). To track the rate of adaptation, we examined the number of generations to the genetic bottleneck measured from generation 1 (Fig. 8**b**). The Full model has the lowest time, followed by the NoHier model. The NoDev and NoCue models reach the genetic bottleneck later than the Full and NoHier models.

We next examined the effectiveness of purifying selection by comparing the decrease in genetic variance between generation 1 and the genetic bottleneck (Fig. 8**c**). The Full model exhibits the largest decrease in genetic variance among all models. The NoCue model exhibits a slightly larger decrease in genetic variance compared to the NoHier and NoDev models. This suggests that hierarchical developmental regulation enhances selection.

We also present the trajectory of projected genotypic value (c.f. Fig. 4) over evolution in the novel environment (Fig. 8**d**). The genotypic value generally increases rapidly when the genetic variance decreases rapidly, indicating strong purifying selection. On the other hand, the genotypic value generally increases slowly when the genetic variance increases slowly, indicating a gradual accumulation of neutral or adaptive mutations. These correlations indicate that the trajectory of the genetic

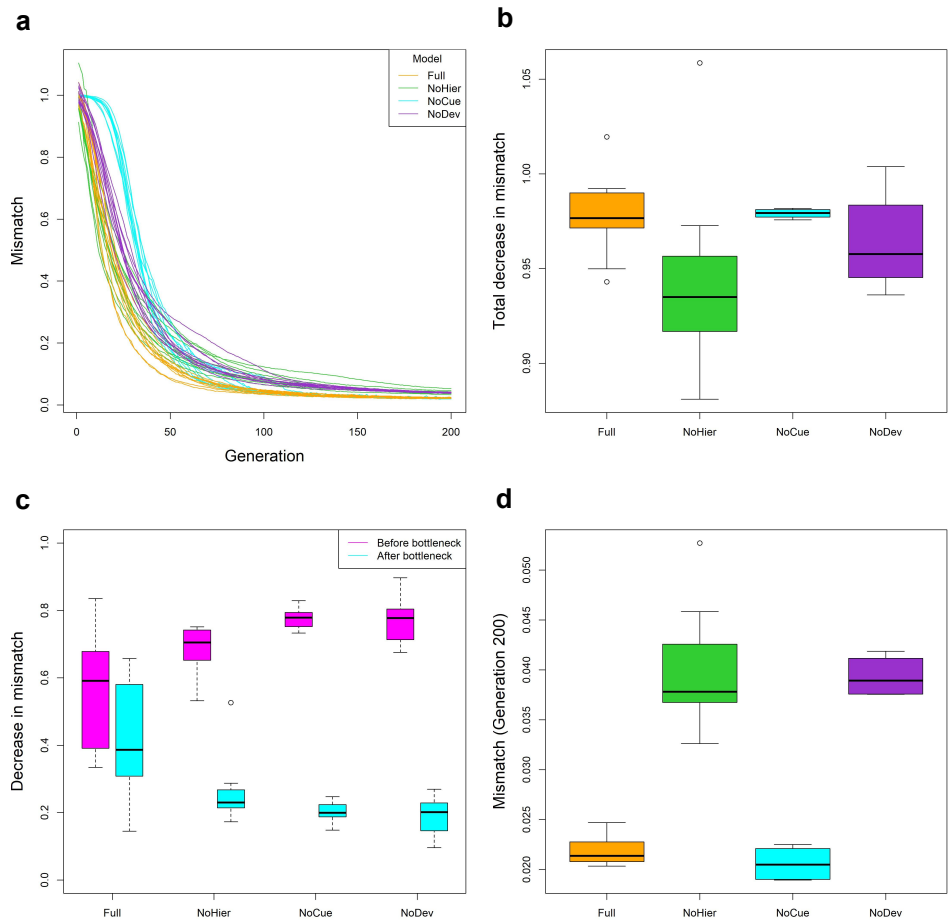

Figure 9: **Adaptive refinement.** **(a)** Trajectory of mismatch between phenotype expressed in novel environment and selective environment over evolution. **(b)** Boxplot of total decrease in mismatch from generation 1 up to generation 200. **(c)** Boxplots of decrease in the mismatch before and after the genetic bottleneck. **(d)** Boxplot of the mismatch at generation 200.

variance is a suitable proxy for studying the change in regulation. Consistent with Fig. 8(**a**), we observe that the Full model exhibits the fastest increase (largest gradient) in genotypic value during the initial phase of evolution, indicating the fastest adaptation. For the NoCue model, the slow increase in genotypic value during the initial phase corresponds to the search for adaptive mutations via genetic drift.

Full model exhibits greatest adaptive refinement

We now compare the effectiveness of adaptive refinement, the increase in fitness in novel environments, between the different models. To do so, we examined the trajectories of the mismatch between the adult phenotype and the selective environment for different models in the novel environments (Fig. 9**a**). All models exhibit decrease in mismatch over evolution, trivially demonstrating that all mod-

els undergo adaptive refinement. All models, except for the NoCue model, exhibit rapid decrease in mismatch immediately during the initial phase of evolution. On the other hand, the mismatch of the NoCue model remains constant for around 25 generations before rapidly decreasing. This delay corresponds to the time required to find adaptive mutations in the novel environment (c.f. Fig. 8). This observation highlights the roles of environmental cues in inducing adaptive plastic phenotype and uncovering cryptic mutations to natural selection, thereby accelerating evolution.

When we compared the total decrease in mismatch among all models from generation 1 to generation 200, the Full and NoCue models exhibit greater decreases in mismatch than the NoHier and NoDev models on average (Fig. 9**b**). The decrease in mismatch for the NoCue model is the most consistent while that for the NoHier model is the least consistent. For the NoHier model, the small decrease in mismatch could be attributed to low initial mismatch from greatest adaptive plastic response (c.f. Fig. 5**a**).

We dissected the decrease in mismatch into the contributions before and after the genetic bottleneck (Fig. 9**c**; see also Fig. 8**a**). The Full model exhibits similar amounts of decrease in mismatch before and after the genetic bottleneck. In contrast, the decrease in mismatch before the genetic bottleneck tends to be significantly greater than that after the genetic bottleneck for all other models. The implications of this behavior is unclear and could be an interesting topic for future studies.

To compare the quality of phenotypes after evolution, we examined the mismatch of the models at generation 200 (Fig. 9**d**). The Full and NoCue models attain a significantly lower value of mismatch at generation 200 compared to the NoHier and NoDev models. This suggests that hierarchical developmental regulation plays an important role in refining phenotype quality. However, the lower mismatch for the NoCue model may be also explained by the absence of environmental noise in developmental regulation.

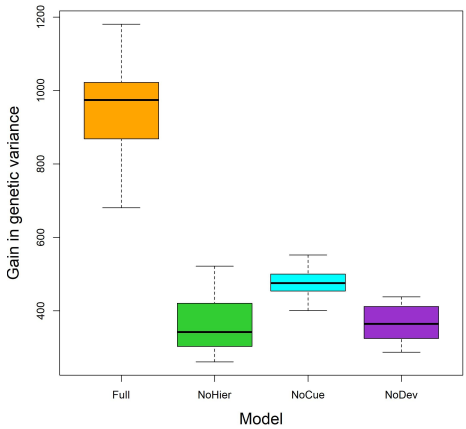

Figure 10: **Accumulation of cryptic mutations**. Boxplot of increase in genetic variance from genetic bottleneck up to generation 200.

Full model accumulates the most mutations after the genetic bottleneck

Uncovering of cryptic genetic variation through plastic response under large environmental changes is one of the core criteria of plasticity-led evolution (12). However, this criterion assumes that cryptic genetic variation has accumulated in the ancestral environment. We compare the accumulation of cryptic mutations between different models by measuring the increase in genetic variance after the genetic bottleneck in the novel environments (Fig. 10). The Full model exhibits a significantly larger increase in genetic variance compared to all the other models. In contrast, the NoHier and NoDev models exhibit the smallest increase in genetic variance on average.

We also observe that the gain in genetic variance after the genetic bottleneck is correlated to the drop in genetic variance before the genetic bottleneck (see Figs. 8 **a,b**). This can be explained by the fact that the length of each epoch is kept constant at 200 generations, so the same amount of cryptic mutations are accumulated in every epoch. Since the accumulation of cryptic mutations is made possible by the robustness of developmental systems (15; 26; 31; 34), we may deduce that the Full model is the most robust of all the discussed models.

Plasticity-led evolution is an intrinsic behavior of developmental networks instead of developmental memory

Watson *et al.* (18) showed that GRNs exploit correlations between traits in formerly adaptive phenotypes to generate novel adaptive phenotypes when subjected to novel environmental cues . As such, they hypothesized that the developmental memory of GRNs should enhance plastic responses, thereby facilitating faster adaptation to novel environments (35). Based on this hypothesis, we trained our models for 40 epochs so that they can acquire developmental memory. We now study how developmental memory of past adaptive phenotypes impacts plasticity-led evolution. As a control, we trained another model with all the features of the Full model but for only one epoch (instead of 40 epochs) before being exposed to novel environments. We name this the *NoTrain* model. We compared the performances of the Full and NoTrain models in light of the Levis-Pfennig criteria of plasticity-led evolution.

To assess adaptive plastic responses and uncovering of cryptic mutations, we compared the projected phenotypes between the Full and NoTrain models in generation 1 (Fig. 11**a**). The ranges of the projected phenotypes are largely overlapping between the two models, suggesting that the difference is not significant. Moreover, the similar range in projected novel phenotype suggests that the effects of cryptic mutations uncovered are about the same for both models.

We further compared the total Pheno-Cue and Pheno-Geno cross-covariances (Fig. 11**b**, left and right vertical axes, respectively) between the Full and NoTrain models but did not find significant differences. The change in regulation, as tracked via the genetic variance in the novel environments (Fig. 11**c**), did not show any significant difference. Finally, we dissected the total decrease in mismatch of the Full and NoTrain models to before and after the genetic bottleneck (c.f. Fig. 9**c**) to compare adaptive refinement between the two models (Fig. 11**d**), again, failing to find any significant difference. However, we note that having (almost) equal fitness contributions before and after the genetic bottleneck is a generic feature of the Full model (i.e. models with environmental cue, hierarchal regulation and developmental process). Although it is not visible in Fig. (11), the genotype-phenotype plots (Supplementary Information) show that the NoTrain model is more overfitted to

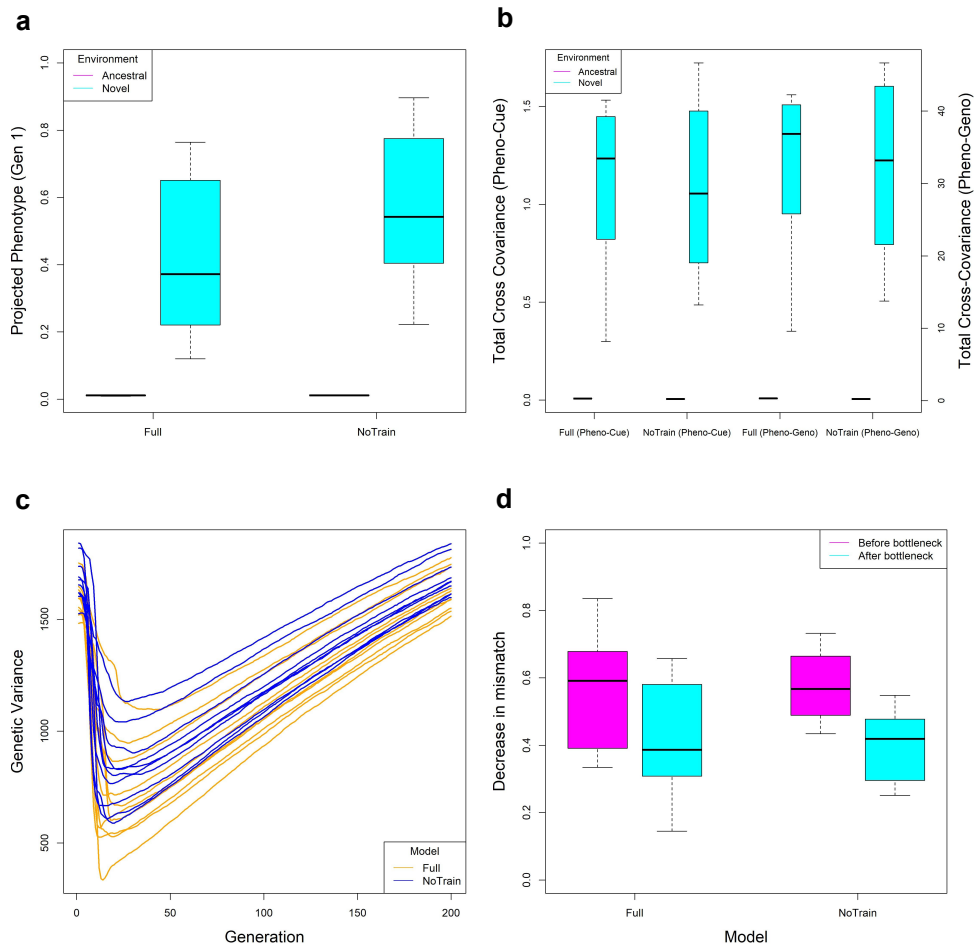

Figure 11: **Effect of training on plasticity-led evolution.** **(a)** Boxplot of projected phenotype in ancestral and novel environment. **(b)** Boxplot of total cross-covariance between phenotype and cue alongside total cross-covariance between phenotype and genome. **(c)** Trajectory of genetic variance. **(d)** Boxplot comparing decrease in mismatch due to change in regulation and adaptive refinement between models.

the ancestral environment than the Full model.

Integrating these results, we conclude that there is no significant contribution to plasticity-led evolution from developmental memory, contrary to the results of Watson *et al.* (18; 35). This discrepancy is due to the absence of strong correlations between traits in our model. Watson *et al.* employed 2-dimensional images as the selected phenotype (18), which have strong correlations between traits. In that context, developmental memory can exploit these correlations to accelerate adaptive evolution. On the other extreme, we do not assume any correlation between traits in our models. In this context, developmental memory may not play as important a role.

Discussion

We have shown that the Full and NoHier models satisfy all the Levis-Pfennig criteria of plasticity-led evolution. In particular, the Full model has additional favorable properties such as amplifying uncovering and accumulation of cryptic mutations, accelerating change in regulation, and undergoing greater adaptive refinement compared to the NoHier model. These observations suggest that environmental cues and the developmental process are essential for plasticity-led evolution, and hierarchical regulation enhances the desirable properties of plasticity-led evolution. These models consistently exhibit plasticity-led evolution over different environments, suggesting that plasticity-led evolution is an intrinsic behavior of these systems. This is not in line with the view that plasticity is explained by genetic variation (1). We discuss the implications of this conflict below.

Contrary to our results, there are studies with natural populations that suggest that plastic response is not always adaptive. For instance, spadefoot toad populations subjected to a dry condition during their larval stage express stunted development resulting in potentially reduced fitness (36). Another example is observed in populations of blue tits that use temperature cues to determine egg-laying periods: due to climate change, adult blue tits now prematurely lay their eggs therefore missing out on the optimal period when the caterpillar population (food source) is abundant (37). In these studies, however, the "environment-as-inducer" does not match with the "environment-as-selector" so it is only natural that the induced phenotypes are not adaptive. Ghalambor et al. (38) introduced a population of guppies previously adapted to a high-predation (HP) environment to a low-predation (Intro) environment and compared the transcript abundance of the introduction populations with that of a population already adapted to a low-predation environment (LP). They claimed that transcription factors associated with initial plasticity are opposite to the direction of adaptive evolution suggesting that non-adaptive plasticity can enhance evolution. However, the "non-adaptive plasticity" by Ghalambor et al. (38) simply means that the genes responsible for the initial plastic response do not coincide with those responsible for later change of regulation, not that the plastic response is non-adaptive with respect to the environmental change. In fact, Fig. 1 of Ghalambor et al. (38) suggests that the

plastic response of the Intro populations is indeed in the same direction as the LP population, hence adaptive.

Developmental bias, the tendency to generate certain kinds of phenotypes more readily than others, has been suggested as a critical mechanism for directing and thereby facilitating evolution (29; 30; 39). We observed that phenotypic variation due to environmental cues is unbiased in adapted environments but is highly biased in novel environments for the Full and NoHier models (Fig. 5**c**). This biased phenotypic variation was found consistently parallel to the direction of environmental changes (Fig. 5**d**). Furthermore, we observe the same behavior for phenotypic variation due to mutations (Figs. 6 **c**,**d**, and 7). These results imply that phenotypic variation due to uncovered mutations is aligned with environmental change, which, in turn, enhances the selection of adaptive mutations (and elimination of maladaptive mutations) in the novel environment. Although the exact causes of this behavior are unclear, we believe it arises from the interplay between environmental cues and the developmental process since the NoCue and NoDev models do not exhibit this behavior.

Most studies on plasticity-led evolution observe the change in regulation through the changes in reaction norms (12; 21; 40–42). However, reaction norms assume that phenotypic plasticity in the studied traits arises from particular mutations that produce particular responses to particular environmental cues. Although reaction norms are useful for studying the evolution of phenotypic plasticity (43), this kind of phenotypic plasticity does not resolve the problem of gradualism implied by the Modern Evolutionary Synthesis. The problem may be resolved if, as proposed above, plasticity-led evolution and therefore change in regulation is independent of particular genetic variation. In other words, evolution *by* plasticity should be studied separately from the evolution *of* plasticity. Here, the evolution *of* plasticity refers to the case where one or a few genes are responsible for particular plastic responses and are therefore subject to natural selection. The evolution *by* plasticity refers to the case where so many genes are involved that plastic responses are considered a generic property of the developmental system so that not plasticity per se, but the resulting phenotypes due to uncovered genetic variation, are subject to natural selection. To validate this hypothesis, it may be helpful to study populations

over many different novel environments and measure all traits subject to natural selection instead of some specific traits (13).

Methods

Convergence of developmental process

To check the convergence of developmental process of an individual, we used the limit of the exponential moving average (EMA) of the phenotype vector $p(s)$. Denote the EMA of the phenotype as the vector $\tilde{p}(s)$ and its variance as the vector $v(s)$. Let $0 < \alpha < 1$ be given as the "step size" of the exponential moving average. In our work we used $\alpha = 1/3$. The values of $\tilde{p}(s)$ and $v(s)$ are recursively updated as follows:

$$\begin{aligned} \tilde{p}_i(s) &= \alpha p_i(s) + (1-\alpha)\tilde{p}_i(s-1), \\ v_i(s) &= (1-\alpha)\{v(s-1) + \alpha[\tilde{p}_i(s-1) - p_i(s)]^2.\} \end{aligned} \tag{8}$$

We say that the phenotype has converged when $\sum_i v_i(s) < 10^{-5}$ for $s \leq 200$ and take the adult phenotype as $\tilde{p}_i(s)$, otherwise, we say that the phenotype does not converge.

Mutation

To randomly introduce mutations during reproduction, we let the mutation rate and matrix density be γ and ρ, respectively, such that both are between 0 and 1. The mutation rate γ represents the proportion of the genome matrix elements to be mutated per reproduction. We mutate the genome of each offspring as follows:

1. Initialize $n = 0$.
2. Sample the number of mutations N from a Poisson distribution where the mean is the product between γ and the genome size. (In our work, we used $\gamma = 0.005$ so we sampled from a Poisson distribution with mean $\lambda = 0.005 \times 200 \times 200 \times 6 = 1200$.)
3. Uniformly select an element in the genome matrix ensemble. The selected element is set to a value of 0 with probability $1 - \rho$, a value of $+1$ with probability $\rho/2$ and -1 with probability $\rho/2$. Increase n by 1.

4. If $n < N$, return to step 3. Else, terminate the process.

Visualizing evolutionary trajectory on genotype-phenotype space

To visualize the evolutionary trajectory of a population, we project the phenotype and genotype of individuals in the population at each generation onto a 2-dimensional genotype-phenotype space. First, the phenotype axis is defined as $\frac{\mathbf{e}_n - \mathbf{e}_a}{\|\mathbf{e}_n - \mathbf{e}_a\|_2^2}$ where $\mathbf{e}_n$ is the first 40 elements of the novel macro-environment, $\mathbf{e}_a$ is the first 40 elements of the ancestral macro-environment and $\|\mathbf{e}_n - \mathbf{e}_a\|_2$ is the Euclidean (L2) distance between $\mathbf{e}_n$ and $\mathbf{e}_a$. We consider only the first 40 out of 200 elements because they correspond to the traits subject to selection. We project the phenotype p of an individual as:

$$\mathbf{p} = (p - \mathbf{e}_a) \cdot \frac{\mathbf{e}_n - \mathbf{e}_a}{\|\mathbf{e}_n - \mathbf{e}_a\|_2^2}. \tag{9}$$

This way, the projected phenotypic values $\mathbf{p}$ of 0 and 1 correspond to phenotypes perfectly adapted to the ancestral and novel environments, respectively.

Next, the genotype axis is defined as follows. Let $\mathbf{G}_{ij}$ be the vectorized genotype matrix of the i-th individual of the j-th generation. Let $\overline{\mathbf{G}}_j = \frac{1}{N}\sum_{i=1}^{N} \mathbf{G}_{ij}$ be the population average genotype vector on the j-th generation. The genotype axis is defined as $\frac{\overline{\mathbf{G}}_{200} - \overline{\mathbf{G}}_1}{\|\overline{\mathbf{G}}_{200} - \overline{\mathbf{G}}_1\|_2^2}$. We project the genotype of the i-th individual of the j-th generation onto a genotype axis as:

$$g_{ij} = (\mathbf{G}_{ij} - \overline{\mathbf{G}}_1) \cdot \frac{\overline{\mathbf{G}}_{200} - \overline{\mathbf{G}}_1}{\|\overline{\mathbf{G}}_{200} - \overline{\mathbf{G}}_1\|_2^2}. \tag{10}$$

This way, projected genotypic values g_{ij} of 0 and 1 correspond to the average genotypes before and after one epoch of evolution in a novel environment, respectively.

Singular value decomposition (SVD) analysis of cross-covariance matrix

We use cross-covariance matrices to study the correlation between selected phenotypes and environmental noise or mutations. Hence, we only consider the first 40

out of 200 elements of phenotype vector, that is, the traits subject to selection. We define the Pheno-Cue cross-covariance matrix as

$$C_{ij}^{\text{Pheno-Cue}} = \frac{1}{N}\sum_{k=1}^{N}(p_{ik} - \overline{p}_i)(e_{jk} - \overline{e}_j) \tag{11}$$

where p_{ik} is the i-th trait of the phenotype vector of the k-th individual, $\overline{p}_i$ is the population average of the i-th trait, e_{jk} is the j-th environmental factor of the k-th individual and $\overline{e}_j$ is the j-th macro-environment factor. We use all 200 elements of the environmental cue vector.

We define the Pheno-Geno cross-covariance matrix as

$$C_{ij}^{\text{Pheno-Geno}} = \frac{1}{N}\sum_{k=1}^{N}(p_{ik} - \overline{p}_i)(\mathbf{G}_{jk} - \overline{\mathbf{G}}_j) \tag{12}$$

where p_{ik} and $\overline{p}_i$ are as defined previously, $\mathbf{G}_{jk}$ is the j-th element of the vectorized genome of the k-th individual and $\overline{\mathbf{G}}_j$ is the population average value of the j-th element of the vectorized genome.

If C_{ij} is the Pheno-Cue or Pheno-Geno cross covariance matrix, then the total cross-covariance is defined as

$$\text{Total cross-covariance} = \sum_i \sum_j C_{ij}^2. \tag{13}$$

This is used in Figs. 5**b** and 6**b**.

To find the principal components of phenotypic variation in response to environmental noise or mutations, we apply singular value decomposition (SVD)(44) on the corresponding cross-covariance matrices. We may apply SVD to any matrix C to obtain orthonormal components as follows.

$$C = U\Sigma V^\top = \sum_i \sigma_i u_i v_i^\top \tag{14}$$

where the superscript $\top$ indicates transpose. In Eq. (14), u_i and v_i are the i-th columns of U and V, respectively, and are called the i-th left and right singular vectors, respectively. Σ is a diagonal matrix where the diagonal elements σ_i are singular values arranged in decreasing order. In the case where C is a Pheno-Cue (or Pheno-Geno) cross-covariance matrix, the left singular vectors correspond to the

principal axes of phenotypic variation in response to the corresponding principal axes (the right singular vectors) of environmental noises (or mutations). The singular values correspond to the cross-covariance between the left and right singular components.

To quantify developmental bias, we used the proportion of the first singular value

$$\frac{\sigma_1^2}{\sum_i \sigma_i^2}. \tag{15}$$

This is used in Figs. 5**c** and 6**c**.

The alignment between the principal axis of phenotypic variation and environmental change is measured by the magnitude of the dot product

$$|u_1 \cdot (\mathbf{e}_n - \mathbf{e}_a)| \tag{16}$$

where $\mathbf{e}_n$ is the novel macro-environment and $\mathbf{e}_a$ is the ancestral macro-environment. This is used in Figs. 5**d** and 6**d**.

Acknowledgments

The authors thank David Marshall and Daphne Teck Ching Lai for helpful comments, and Haziq Jamil for stimulating discussion. E.T.H.N. was supported by UBD Bursary Award.

Author contributions

A.R.K. conceived the models and ran preliminary simulations. E.T.H.N. ran large-scale simulations and collected the data. E.T.H.N. and A.R.K. designed the work plan, wrote the computer programs, analyzed the data, and wrote the manuscript.

Competing interests

The authors declare no competing interests.

Availability of computer code

Computer code is provided in the GitHub repository: https://github.com/arkinjo/evodevo/tree/paper1

References

[1] Futuyma DJ. How does phenotypic plasticity fit into evolutionary theory? In: Pfennig DW, editor. Phenotypic Plasticity & Evolution. Boca Raton, FL: CRC Press; 2021. p. 349–366.

[2] Crow JF, Kimura M. An introduction to population genetics theory. New York, USA: Harper and Row Publishers; 1970.

[3] Falconer DS, Mackay TFC. Introduction to Quantitative Genetics. 4th ed. Harlow: Pearson; 1996.

[4] Ng ETH, Kinjo AR. Computational modelling of plasticity-led evolution. Biophys Rev. 2022;14:1359–1367. doi:10.1007/s12551-022-01018-5.

[5] Nishikawa K, Kinjo AR. Cooperation between phenotypic plasticity and genetic mutations can account for the cumulative selection in evolution. Biophysics. 2014;10:99–108. doi:10.2142/biophysics.10.99.

[6] West-Eberhard MJ. Developmental plasticity and evolution. New York: Oxford University Press; 2003.

[7] Gilbert SF, Epel D. Ecological Developmental Biology: Integrating Epigenetics, Medicine, And Evolution. Sunderland, MA: Sinauer Associates; 2009.

[8] Pfennig DW. Phenotypic plasticity & evolution: causes, consequences, controversies. Taylor & Francis; 2021.

[9] Waddington CH. Genetic assimilation of an acquired character. Evolution. 1953;7:118–126. doi:10.2307/2405747.

[10] Nijhout HF, Kudla AM, Hazelwood CC. Genetic assimilation and accommodation: models and mechanisms. Curr Top Dev Biol. 2021;141:337–369. doi:10.1016/bs.ctdb.2020.11.006.

[11] Nishikawa K, Kinjo AR. Mechanism of evolution by genetic assimilation: Equivalence and independence of genetic mutation and epigenetic modulation in phenotypic expression. Biophys Rev. 2018;10(2):667–676. doi:10.1007/s12551-018-0403-x.

[12] Levis NA, Pfennig DW. Evaluating 'plasticity-first'evolution in nature: key criteria and empirical approaches. Trends Ecol Evol. 2016;31(7):563–574. doi:10.1016/j.tree.2016.03.012.

[13] Kovaka K. Underdetermination and evidence in the developmental plasticity debate. Brit J Phil Sci. 2019;70:127–152. doi:10.1093/bjps/axx038.

[14] Laland K, Uller T, Feldman M, Sterelny K, Müller GB, Moczek A, et al. Does evolutionary theory need a rethink? Nature. 2014;514(7521):161–164. doi:10.1038/514161a.

[15] Bergman A, Siegal ML. Evolutionary capacitance as a general feature of complex gene networks. Nature. 2003;424(6948):549–552. doi:10.1038/nature01765.

[16] Davidson E, Erwin D. Gene Regulatory Networks and the Evolution of Animal Body Plans. Science. 2006;311:796–800. doi:10.1126/science.1113832.

[17] Peter IS, Davidson EH. Evolution of gene regulatory networks controlling body plan development. Cell. 2011;144(6):970–985.

[18] Watson RA, Wagner GP, Pavlicev M, Weinreich DM, Mills R. The evolution of phenotypic correlations and "developmental memory". Evolution. 2014;68(4):1124–1138. doi:10.1111/evo.12337.

[19] Nagata S, Kikuchi M. Emergence of cooperative bistability and robustness of gene regulatory networks. PLoS Comput Biol. 2020;16(6):e1007969.

[20] Kaneko T, Kikuchi M. Evolution enhances mutational robustness and suppresses the emergence of a new phenotype: A new computational approach for studying evolution. PLoS Comput Biol. 2022;18(1):e1009796. doi:10.1371/journal.pcbi.1009796.

[21] Lande R. Adaptation to an extraordinary environment by evolution of phenotypic plasticity and genetic assimilation. J Evol Biol. 2009;22(7):1435–1446. doi:10.1111/j.1420-9101.2009.01754.x.

[22] Lee U, Mortola EN, Kim EJ, Long M. Evolution and maintenance of phenotypic plasticity. Biosystems. 2022;222:104791. doi:10.1016/j.biosystems.2022.104791.

[23] Xue B, Sartori P, Leibler S. Environment-to-phenotype mapping and adaptation strategies in varying environments. Proc Natl Acad Sci USA. 2019;116(28):13847–13855. doi:10.1073/pnas.1903232116.

[24] Wagner A. Does evolutionary plasticity evolve? Evolution. 1996;50(3):1008–1023. doi:10.1111/j.1558-5646.1996.tb02342.x.

[25] Espinosa-Soto C, Martin OC, Wagner A. Phenotypic plasticity can facilitate adaptive evolution in gene regulatory circuits. BMC Evol Biol. 2011;11(1):1–14. doi:10.1186/1471-2148-11-5.

[26] Espinosa-Soto C, Martin OC, Wagner A. Phenotypic robustness can increase phenotypic variability after nongenetic perturbations in gene regulatory circuits. J Evol Biol. 2011;24(6):1284–1297. doi:10.1111/j.1420-9101.2011.02261.x.

[27] Kouvaris K, Clune J, Kounios L, Brede M, Watson RA. How evolution learns to generalise: Using the principles of learning theory to understand the evolution of developmental organisation. PLoS Comput Biol. 2017;13(4):e1005358. doi:10.1371/journal.pcbi.1005358.

[28] Espinosa-Soto C, Hernández U, Posadas-García YS. Recombination facilitates genetic assimilation of new traits in gene regulatory networks. Evol Dev. 2021;23(5):459–473. doi:10.1111/ede.12391.

[29] Draghi JA, Whitlock MC. Phenotypic plasticity facilitates mutational variance, genetic variance, and evolvability along the major axis of environmental variation. Evolution. 2012;66(9):2891–2902. doi:10.1111/j.1558-5646.2012.01649.x.

[30] Uller T, Moczek AP, Watson RA, Brakefield PM, Laland KN. Developmental bias and evolution: A regulatory network perspective. Genetics. 2018;209(4):949–966. doi:10.1534/genetics.118.300995.

[31] Siegal ML, Bergman A. Waddington's canalization revisited: developmental stability and evolution. Proc Natl Acad Sci USA. 2002;99(16):10528–10532.

[32] Brun-Usan M, Zimm R, Uller T. Beyond genotype-phenotype maps: Toward a phenotype-centered perspective on evolution. BioEssays. 2022;44(9):2100225.

[33] Waddington CH. The strategy of the genes. London: George Allen & Unwin Ltd.; 1958.

[34] Ehrenreich IM, Pfennig DW. Genetic assimilation: a review of its potential proximate causes and evolutionary consequences. Ann Bot. 2016;117(5):769–779. doi:10.1093/aob/mcv130.

[35] Watson RA, Szathmáry E. How can evolution learn? Trends Ecol Evol. 2016;31(2):147–157. doi:10.1016/j.tree.2015.11.009.

[36] Merilä J, Laurila A, Lindgren B. Variation in the degree and costs of adaptive phenotypic plasticity among Rana temporaria populations. J Evol Biol. 2004;17(5):1132–1140. doi:10.1111/j.1420-9101.2004.00744.x.

[37] Bonamour S, Chevin LM, Charmantier A, Teplitsky C. Phenotypic plasticity in response to climate change: the importance of cue variation. Philos Trans R Soc Lond, B, Biol Sci. 2019;374(1768):20180178. doi:10.1111/j.1420-9101.2004.00744.x.

[38] Ghalambor CK, Hoke KL, Ruell EW, Fischer EK, Reznick DN, Hughes KA. Non-adaptive plasticity potentiates rapid adaptive evolution of gene expression in nature. Nature. 2015;525(7569):372–375. doi:10.1098/rstb.2018.0178.

[39] Noble DW, Radersma R, Uller T. Plastic responses to novel environments are biased towards phenotype dimensions with high additive genetic variation. Proc Natl Acad Sci USA. 2019;116(27):13452–13461. doi:10.1073/pnas.1821066116.

[40] Scheiner SM. Genetics and evolution of phenotypic plasticity. Annu Rev Ecol Evol Syst. 1993; p. 35–68. doi:10.2307/2097172.

[41] Scheiner SM, Barfield M, Holt RD. The genetics of phenotypic plasticity. XVII. Response to climate change. Evol Appl. 2020;13(2):388–399. doi:10.1111/eva.12876.

[42] Levis NA, Pfennig DW. Innovation and diversification via plasticity-led evolution. In: Pfennig DW, editor. Phenotypic Plasticity & Evolution. Boca Raton, FL: CRC Press; 2021. p. 211–240.

[43] Pigliucci M. Evolution of phenotypic plasticity: where are we going now? Trends Ecol Evol. 2005;20:481–486. doi:10.1016/j.tree.2005.06.001.

[44] Yanai H, Takeuchi K, Takane Y. Projection Matrices, Generalized Inverse Matrices, and Singular Value Decomposition. New York, NY: Springer; 2011.